ISTITUTO NAZIONALE DI FISICA NUCLEARE
Laboratori Nazionali di Frascati

LNF-80/39(R)
14 Luglio 1980

P. Barreau, M. Bernheim, M. Brussel, G. P. Capitani, E. De Sanctis, J. M. Finn, S. Frullani, F. Garibaldi, E. Jans, J. Morgenstern, J. Mougey, D. Royer, D. Tarnowski, S. Turck Chieze and P. Vernin: STATUS REPORT ON THE STUDY OF FEASIBILITY OF THE (e, e'n) REACTIONS IN THE HE 1 ROOM OF THE SACLAY LINEAR ACCELERATOR LABORATORY.

Servizio Documentazione
dei Laboratori Nazionali di Frascati

INFN - Laboratori Nazionali di Frascati
Servizio Documentazione

LNF-80/39(R)
14 Luglio 1980

STATUS REPORT ON THE STUDY OF FEASIBILITY OF THE (e, e'n) REACTIONS IN THE HE 1 ROOM OF THE SACLAY LINEAR ACCELERATOR LABORATORY.

G. P. Capitani, E. De Sanctis
INFN - Laboratori Nazionali di Frascati, Frascati.

S. Frullani, F. Garibaldi
Istituto Superiore di Sanità, Laboratorio delle Radiazioni, and INFN - Sezione Sanità, Roma.

P. Barreau, M. Bernheim, J. M. Finn, J. Morgenstern, J. Mougey, D. Royer, D. Tarnowski, S. Turck-Chieze, P. Vernin
Départment de Physique Nucléaire et Hautes Energies, Centre d'Etudes Nucléaires de Saclay, Gif-sur-Yvette, France.

E. Jans
Instituut voor Kernphysisch Onderzoek, Amsterdam, The Netherlands.

M. Brussel
Physics Department, University of Illinois, Urbana, Illinois, USA.

1. - INTRODUCTION.

In the course of 1979 the "Comité des expériences de l'ALS" assigned us 12 shifts from July 16 to July 20 in order to collect information on the possibility of measuring (e, e'n) reactions in HE 1 as outlined in our intent letter no. 102[1].

This paper reports on the first two items of that letter: a) on measurements of the singles counting rate on the neutron arm, and b) on the possibility of subtracting accidental coincidences from the time of flight spectra.

In Section 2 the experimental set-up is described. Section 3 concerns point a) above. Section 4 is devoted to point b), finally, in Section 5, a preliminary evaluation of the time needed to perform some (e, e'n) experiment on light nuclei is given.

2. - EXPERIMENTAL SET-UP.

The Linac operating conditions during the measurements were:

electron energy	~ 500 MeV
repetition rate	~ 500 Hz
duty cycle	1 %
average current	1 - 2 μA.

The available (e, e'p) - group liquid deuterium target (250 mg/cm^2 thick) was used. It consists of a 1.5 cm diameter stainless steel cylinder with wall 0.002 cm thick.

A sketch of the experimental set-up is shown in Figs. 1 and 2. The neutrons were detected by the liquid scintillator counter N2, (NE 213 in a cylindrical cell of 15 cm diameter and 10 cm thick), in anticoincidence with the N1 plastic scintillator counter (NE 102 A). The two counters were placed on the platform of the 600 spectrometer behind the magnet, and surrounded by massive shielding consisting of 25 cm thick iron and 10-20 cm thick lead (see Fig. 2). Neutrons coming from the target pass through two holes (ϕ = 10 cm), the first in the magnet yoke of the spectrometer and the second in the front wall of the shielding. The distance between N2 and the target was 5 m.

Data were collected using the 600 spectrometer diaphragm no 1, which defines a solid angle of 0.16 msr. This corresponds to about a half of the solid angle defined by the magnet yoke hole.

The values chosen for the solid angle and for the beam current were limited essentially by the maximum

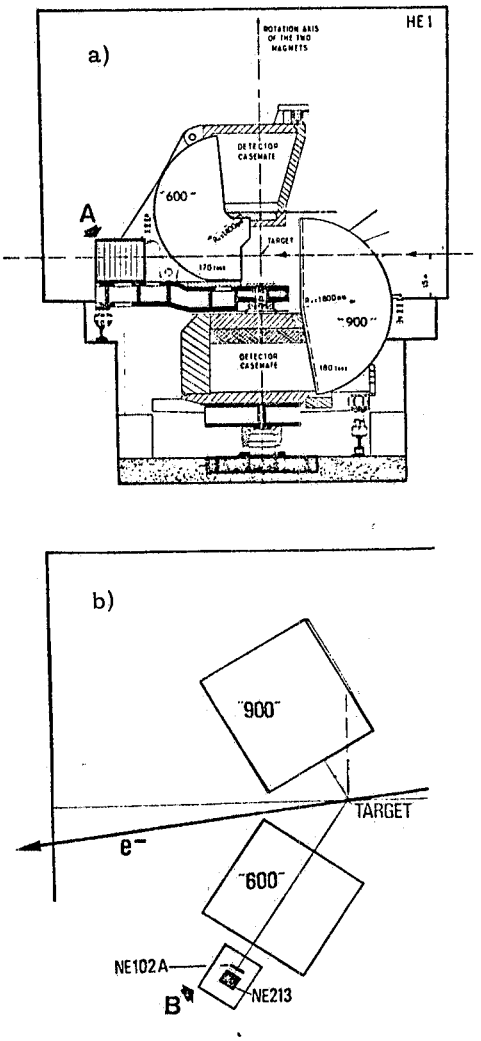

FIG. 1 - Experimental set-up: vertical a) and horizontal b) sections.

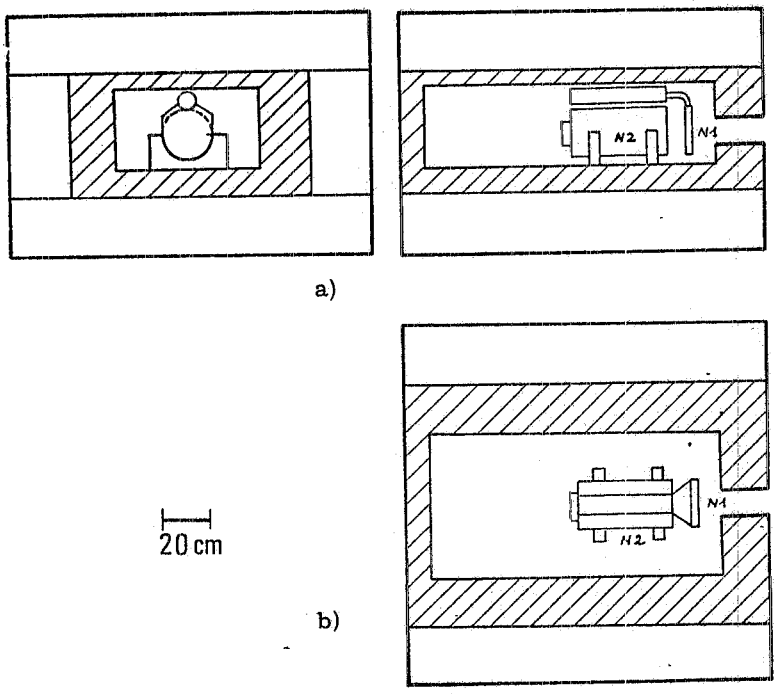

FIG. 2 - Enlarged view of the neutron detector assembly: vertical a) (A in Fig. 1a) and horizontal b) (B in Fig. 1b) sections.

counting rate acceptable by the data acquisition system. This system required a discrimination between neutrons and photons.

For the coincidence measurements the electrons were detected in the 900 spectrometer requiring a coincidence between the two plastic counter arrays ("R" and "Y") of its detection system[2].

In Fig. 3 the electronic block diagram is given. The signal from N2 is divided into three parts: one is used to generate the main gate for the acquisition (a fourfold coincidence - unit C of Fig. 3 - with the beam synchro signal, the CAMAC ready pulse, and the electron arm signal); two others are used for the pulse shape discrimination (P. S. D.), according to the scheme given in Fig. 4[3]. The analog to digital converter measures the shadowed areas. Each event was registered on a magnetic tape and analysed on-line with the SADE program[4]. SADE permits one to present on a video display unit (VT 15) spectra conditioned by various requirements (energy thresholds, neutron-gamma discrimination, coincidence or anticoincidence with N1 signal, etc.) of the fast and slow lines of the N2 signal.

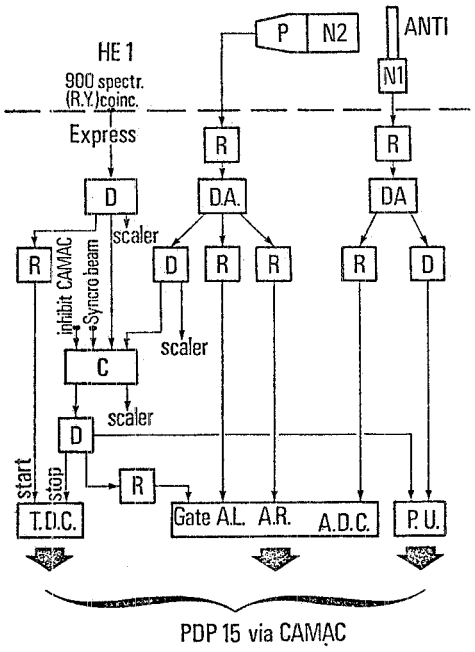

FIG. 3 - Electronic block diagram.

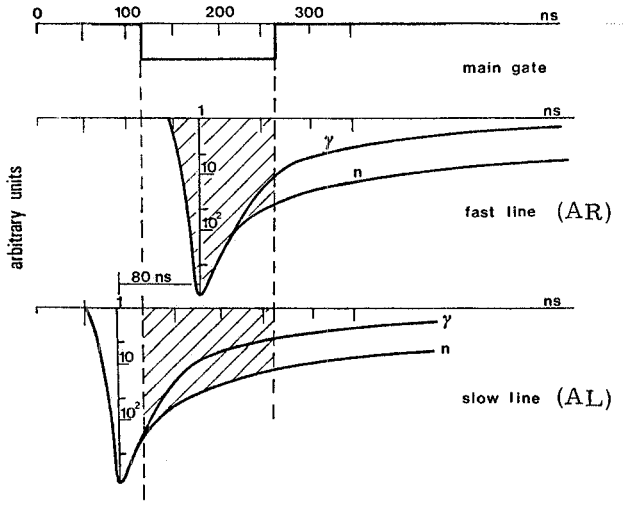

FIG. 4 - Time relationship among the pulse forms in our PSD system.

3. - SINGLE ARM MEASUREMENTS.

Measurements have been taken in the experimental conditions given in Table I where the employed symbols have the following meaning:

0 : is for liquid deuterium in the cell, and a 5 mm lead foil in front of N1;

⊠ : same conditions as 0 with 10.5 cm lead brick added in front of N1;

T.V. : same conditions as 0 except that liquid deuterium was not in the cell.

The values of the total N2 counting rate per 10^{-8}C, N, and of the evaluated mean number of events per beam pulse, $\langle m \rangle$, are given in Table II. $\langle m \rangle$ is evaluated because the acquisition system as used does not accept more than 1 event per beam pulse. Assuming a Poisson distribution for m, the probability P(0) of absence of

TABLE I (see text for explanation).

Average current	Neutron angle detection ϑ_n(°)	Experimental condition		
1 μA	40		⊠	T.V.
	45	0	⊠	
	55	0	⊠	
	65	0	⊠	
2 μA	40		⊠	T.V.
	45	0	⊠	T.V.
	55	0	⊠	T.V.
	65	0	⊠	T.V.

TABLE II - N is the N2 counting rate per 10^{-8}C ; $\langle m \rangle$ is the mean number of events per beam pulse , F is the total charge collected by the Faraday cup.

Experimental conditions	ϑ_n (°)	N 10^8	Average current (μA)	$\langle m \rangle$	F(10^{-8}C)
0	45	~22	1 2	4.9 ± 0.5 10	11594 25573
0	55	5.45	1 2	1.31 ± 0.02 2.52 ± 0.05	10370 17006
0	65	3.65	1 2	0.86 ± 0.01 1.57 ± 0.02	20015 31790
⊠	40	2.22	1 2	0.54 ± 0.01 1.08 ± 0.01	25622 28712
⊠	45	1.94	1 2	0.45 ± 0.01 0.87 ± 0.01	28991 29489
⊠	55	1.56	1 2	 0.73 ± 0.01	28861 34164
⊠	65	1.27	1 2	0.33 ± 0.01 0.59 ± 0.01	48444 50356
T.V.	40	7.46	1 2	2.12 ± 0.04 4.03 ± 0.26	8088 19628
T.V.	45	4.56	2	2.49 ± 0.04	19796
T.V.	55	2.65	2	1.56 ± 0.02	30373
T.V.	65	1.9	2		33017

events in a beam pulse is : $P(0) = e^{-\langle m \rangle} = 1 - N \cdot F/n$ (where n is the number of beam pulses). Thus $\langle m \rangle = \ln [1/(1 - N \cdot F/n)]$. From Table II it is seen that both quantities m and N increase as ϑ_n becomes smaller.

In Figs. 5, 6 and 7 the corresponding discrimination curves between neutrons and gammas obtained for a threshold value of 7.2 MeVee are given. One sees that the discrimination becomes worse as m becomes greater : but it is always satsfactory. By using these curves we have obtained the values given in Table III for the neutron and photon contributions to the total counting

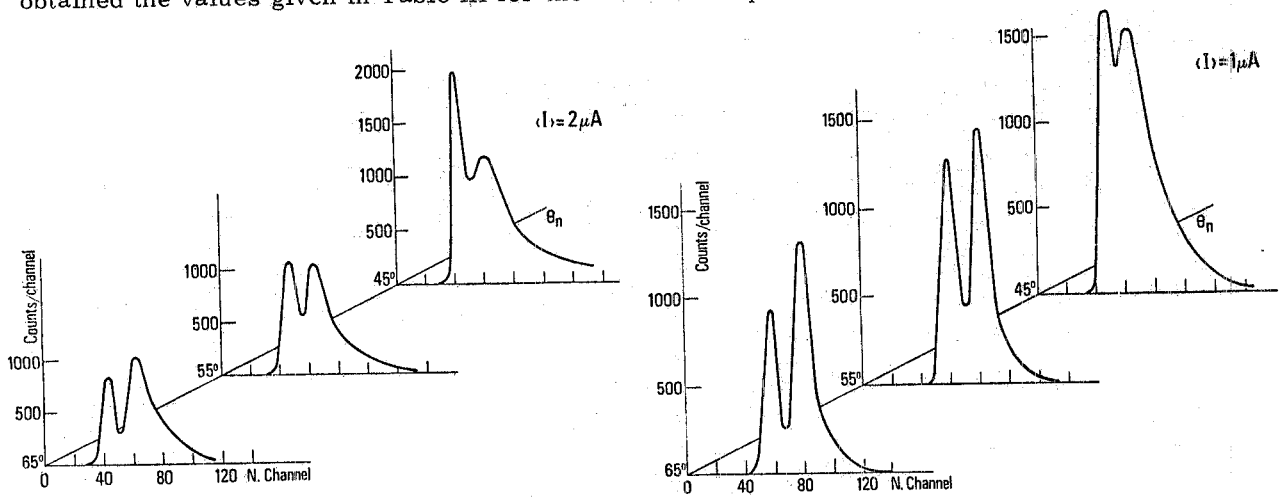

FIG. 5 - Neutron-photon discrimination plots for experimental condition 0.

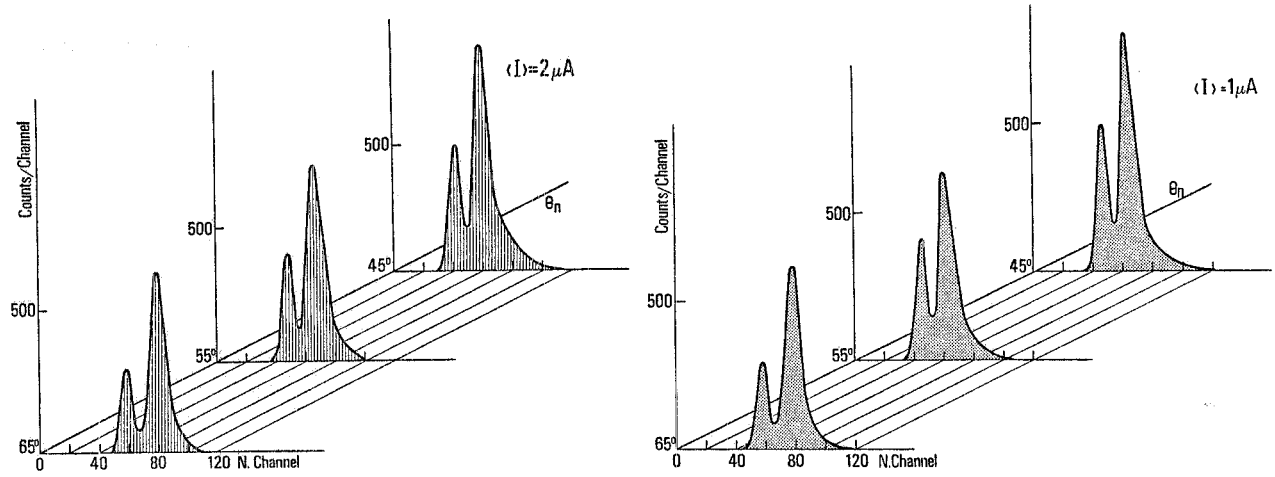

FIG. 6 - Neutron-photon discrimination plots for experimental condition ⊠.

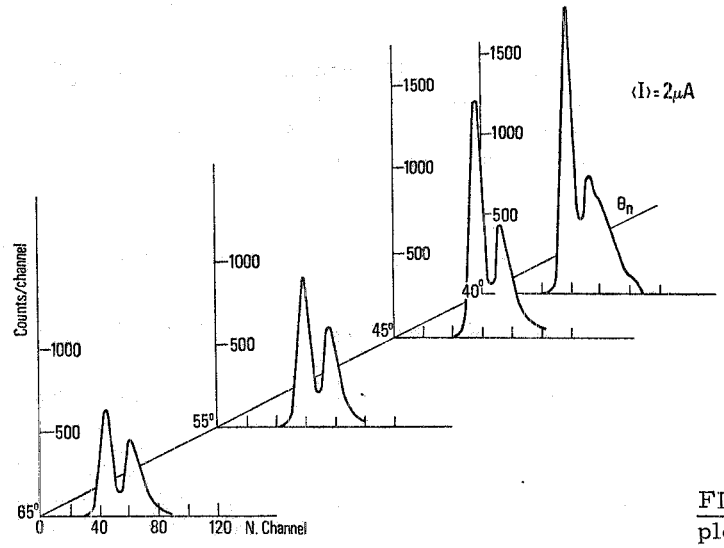

FIG. 7 - Neutron-photon discrimination plots for experimental condition T. V.

TABLE III - Neutron (n) and photon (γ) contributions to the total N2 counting rate for the given threshold values, s.

Experimental condition	ϑ_n (°)	Counts / Coulomb (x 10^8)					
		s = 7.2 MeVee		s = 14.4 MeVee		s = 21.6 MeVee	
		n	γ	n	γ	n	γ
0	65	0.36 ± 0.02	0.20 ± 0.01	0.120 ± 0.005	0.030 ± 0.001	0.070 ± 0.003	0.013
0	55	0.47 ± 0.03	0.25 ± 0.02	0.16 ± 0.01	0.040 ± 0.002	0.085 ± 0.005	0.016
0	45	0.82 ± 0.10	0.44 ± 0.06	0.22 ± 0.03	0.055 ± 0.007	0.10 ± 0.01	0.020 ± 0.002
⊠	65	0.150 ± 0.006	0.050 ± 0.002	0.066 ± 0.002	---	0.040 ± 0.001	---
⊠	55	0.180 ± 0.007	0.070 ± 0.003	0.080 ± 0.003	---	0.049 ± 0.001	---
⊠	45	0.220 ± 0.009	0.080 ± 0.003	0.110 ± 0.004	---	0.068 ± 0.002	---
⊠	40	0.230 ± 0.009	0.090 ± 0.006	0.120 ± 0.004	---	0.070 ± 0.003	---
T.V.	65	0.120 ± 0.006	0.110 ± 0.006	0.054 ± 0.002	0.003 ± 0.0001	0.034 ± 0.001	---
T.V.	55	0.16 ± 0.01	0.15 ± 0.01	0.084 ± 0.005	0.005 ± 0.0002	0.050 ± 0.001	---
T.V.	45	0.20 ± 0.01	0.26 ± 0.02	0.09 ± 0.01	0.017 ± 0.0005	0.056 ± 0.002	---
T.V.	40	0.23 ± 0.02	0.39 ± 0.03	0.10 ± 0.02	0.025 ± 0.001	0.060 ± 0.002	0.004

rate. In Fig. 8 these values together with indications of the contributions from the target and from the deuterium for three threshold values are reported.

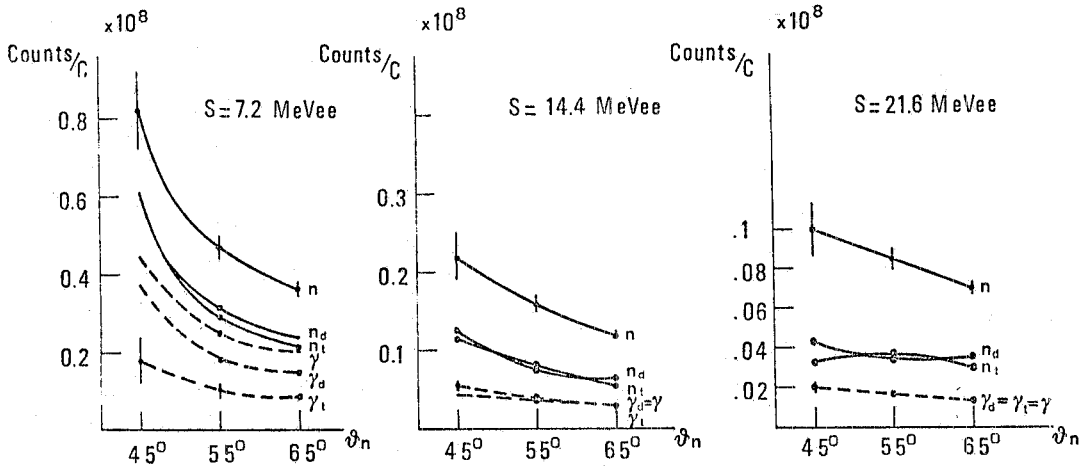

FIG. 8 - Neutron (n) and photon (γ) contributions to the total N2 counting rate per Coulomb for the given threshold values. n_d, n_t (γ_d, γ_t) are respectively neutrons (photons) from the deuteron and from the target. For a sake of simplicity error bars are given only for one neutron (photon) curve: for the other two they have the same absolute value.

As a summary we can say that:

- the neutrons from the target are come essentially from the deuteron, the contribution from the cell walls being negligible;
- the photon spectrum has a low-energy room-background component which can be removed with a threshold of 14.4 MeVee;
- the ratio n_d/γ_d between neutrons and photons coming from the deuterium does not change with the angle ϑ_n or with the threshold; its value is about 0.5.

TABLE IV - Total N2 counting rates from deuterium, N_d, from the target, N_t, and from the room N_r.

ϑ_n	N_d = (0-T.V.)	N_t = (0-⊠)	N_r = ⊠
45°	17.4 (79%)	20 (91%)	1.94 (9%)
55°	2.8 (51%)	3.84 (71%)	1.56 (29%)
65°	1.75 (48%)	2.38 (65%)	1.27 (35%)

Finally in Table IV the total N2 counting rates (neutrons + photons) from deuterium (N_d), from the target area (N_t) and from the room (N_r) at three neutron angles ϑ_n and for a threshold of 3 MeVee, are given. Figures in parenthesis give the percentage relative to the counting rate in condition 0. From the Table we see that N_r is less important in percentage for smaller angles (~10%) and that it grows up to a 35 % of the signal for $\vartheta_n = 65°$.

We hope that by using a more careful shielding it will be possible to make this contribution negligible.

4. - COINCIDENCE MEASUREMENTS.

Measurements have been made in the two kinematical conditions given in Table V.

The spectra obtained in the fast line together with the contribution from neutral (neutrons and photons) and charged components, are given in Fig. 9. In the total and charged component spectra, two peaks, due to electron-positron pair production on the collimator walls and

TABLE V - D(e, e'n)p kinematical conditions. The used symbols have the following meaning: p = momentum; T = kinetic energy; ϑ = ejection angle; $\Delta\Omega$ = solid angle; q^2 = momentum transfer; Δp = momentum acceptance; p_R = initial neutron momentum. The suffixes n and e denote neutron and electron respectively.

Average current (μA)	p_e (MeV/c)	$p_{e'}$ (MeV/c)	$\Delta p_{e'}$ (MeV/c)	$\vartheta_{e'}$ (°)	$\Delta\Omega_{e'}$ (msr)	p_n (MeV/c)	T_n (MeV)	ϑ_n (°)	$\Delta\Omega_n$ (msr)	p_R (MeV/c)	q^2 (fm^{-2})
1 2	515	437.5	35.0	46.6	4.85	383.5	75.2	56.0	0.16	0	3.62
2	515	437.0	35.0	44.0	4.85	383.5	75.2	60.0	0.16	30	3.24

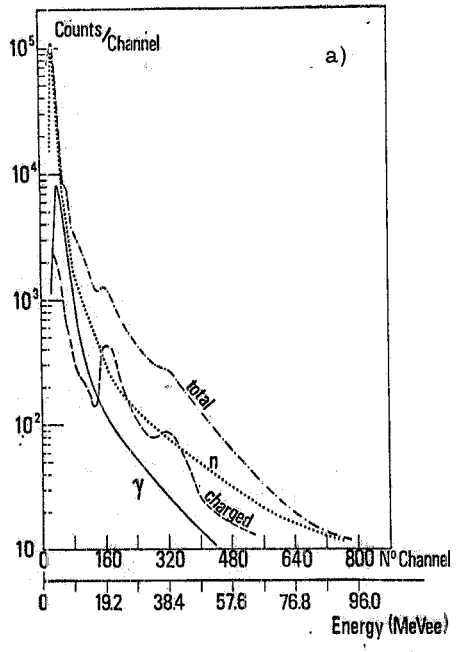

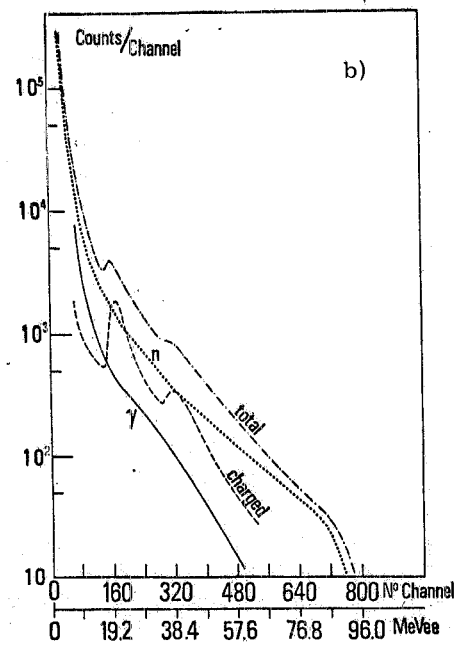

FIG. 9 - Fast line amplitude spectra for the two kinematical conditions:
a) p_R = 0 MeV/c; b) p_R = 30 MeV/c.

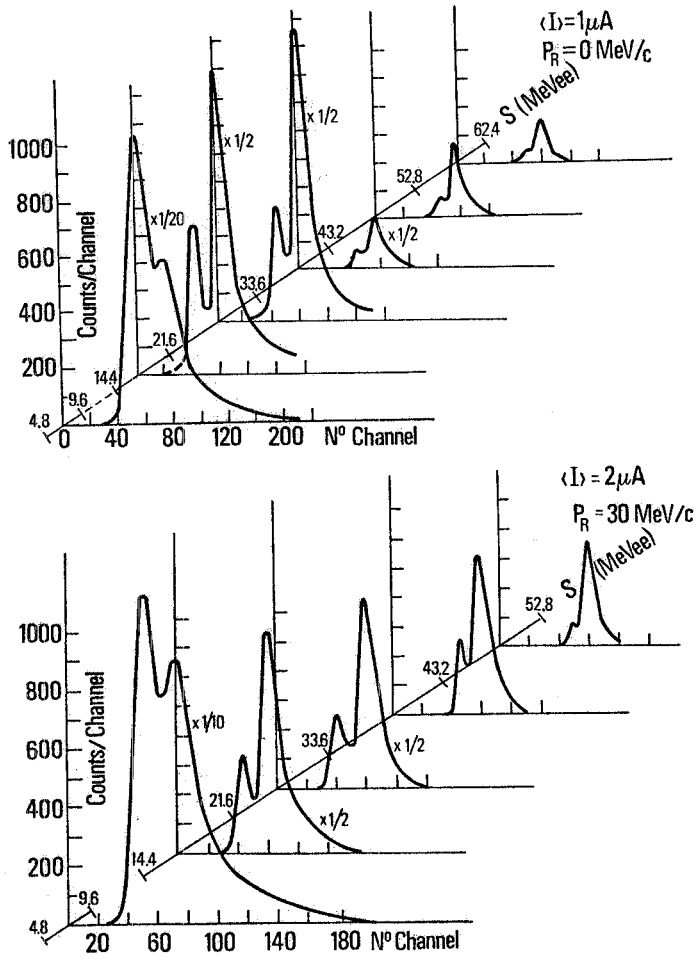

FIG. 10 - Neutron-photon discrimination plots for coincidence measurements for different threshold regions s.

on the 5 mm thick lead foil in front of N1 respectively appear at 20 MeVee and 40 MeVee. The photon spectrum is equal to zero for energies greater than 58 MeVee, as is shown in an even more evident way in Fig. 10, where the discrimination plots for adjacent threshold regions in the fast lines are given. From these plots one finds quite good discrimination for threshold values ≥ 14.4 MeVee. (Actually from other plots, not given here, the discrimination curves are quite good even for threshold value down to 7.2 MeVee).

The time of flight spectra between electrons and N2 events are shown in Fig. 11 : the line $(n+\gamma)$ refers to all the signals in the N2 counter, those labelled n refer only to the signals regarded as due to neutrons (according to the discrimination curves previously shown) for three

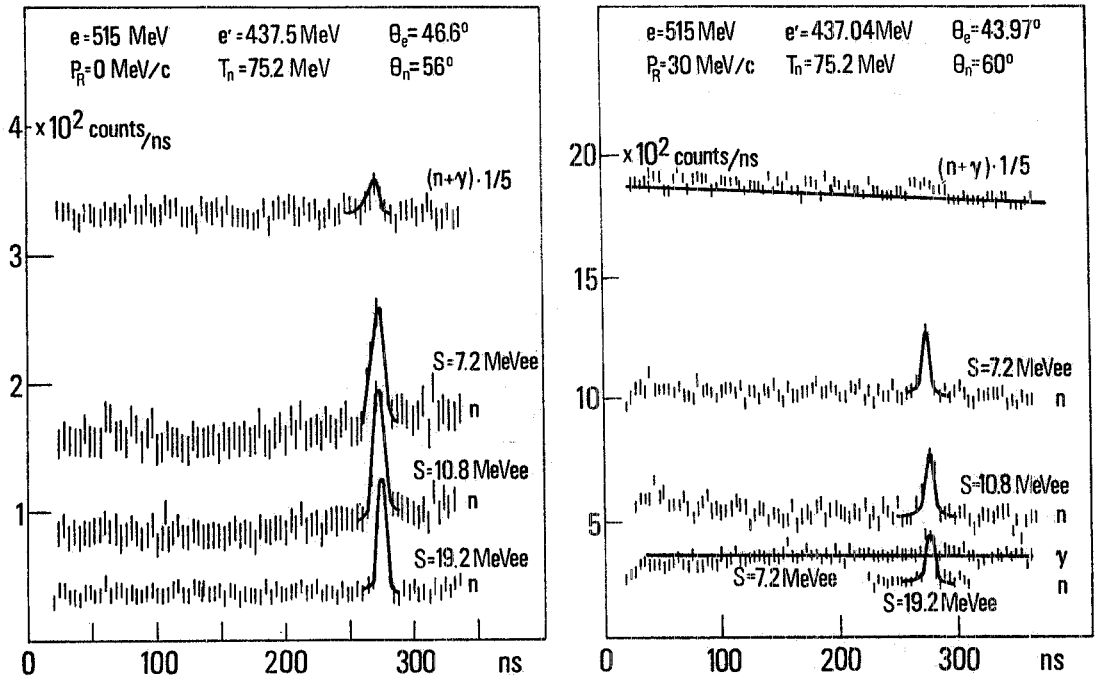

FIG. 11 - Time of flight spectra for the two kinematical conditions given and for the three threshold values s.

different threshold values. The peak of neutrons from the deuteron with 16-20 ns full width appears on a flat background of accidental coincidences. The amount of accidentals under the peak is estimated from the two adjacent regions of the spectrum : the signal to noise ratio varies from 0.14 to 1.0 depending on the threshold and on the beam current values. In Table VI the measured coincidence counting rates per Coulomb together with the evaluated ones are given. The formula used is :

$$N(e, e'n) = N_o \frac{t}{A} \eta \frac{d\sigma}{d\Omega_e d\Omega_n dp_e} \Delta\Omega_e \Delta\Omega_n \Delta p_e ,$$

where :

N_o is the number of incoming electrons ;

t/A is the number of target neutrons per cm^2 $(A = 2)$;

η is the neutron detection efficiency ; the values used, which were obtained by a Monte Carlo[5] calculation, are given in the last line of Table VI ;

$\frac{d\sigma}{d\Omega_e d\Omega_n dp_e} \Delta\Omega_n \Delta p_e = C \frac{d\sigma}{d\Omega_e} \varrho(p_R)$, where C is a kinematical factor, $d\sigma/d\Omega_e$ is the free electron-neutron cross section, and $\varrho(p_R)$ is the probability of finding a neutron with momentum p_R. Assuming for ϱ the Hulten function, we have $\varrho(0 \text{ MeV/c}) = 2\,\varrho(30 \text{ MeV/c}) =$

$= 1.62 \times 10^{-6}$ (MeV/c)$^{-3}$. Following Bounin[6] it results $C \frac{d\sigma}{d\Omega_e} = 1.99 \times 10^{-26}$ MeV^{2}cm^2/sr^2 for $p_R = 0$ MeV/c, and 2.32×10^{-26} MeV^{2}cm^2/sr^2 for $p_R = 30$ MeV/c;

$\Delta\Omega_e$, $\Delta\Omega_n$ are electron and neutron solid angles;

Δp_e is electron momentum acceptance.

TABLE VI - Measured and evaluated coincidence counting rates. Figures in squared parentheses are the true to accidental ratio.

	I	p_r	Counts per Coulomb		
	(μA)	(MeV/c)	s = 7.2 MeVee	s = 10.8 MeVee	s = 19.2 MeVee
experimental	1	0	$(3.2 \pm 0.3) \times 10^4$ [0.27]	$(2.8 \pm 0.3) \times 10^4$ [0.5]	$(2.1 \pm 0.2) \times 10^4$ [1.0]
	2	0	$(3.3 \pm 0.5) \times 10^4$ [0.15]	$(2.7 \pm 0.4) \times 10^4$ [0.26]	$(1.8 \pm 0.2) \times 10^4$ [0.5]
	2	30	$(2.4 \pm 0.3) \times 10^4$ [0.14]	$(2.1 \pm 0.2) \times 10^4$ [0.30]	$(1.4 \pm 0.2) \times 10^4$ [0.47]
theoretical	1	0	3.67×10^4	3.02×10^4	1.96×10^4
	2	0	3.67×10^4	3.02×10^4	1.96×10^4
	2	30	2.14×10^4	1.76×10^4	1.14×10^4
ε_n			0.090	0.074	0.048

In Table VI the true to accidental ratio is given in squared parentheses. As it is shown, the agreement between measured and evaluated coincidences is quite satisfactory.

5. - COMMENTS.

In this section some evaluations of the counting rates and, for a given accuracy, of the machine time required for two different measurements using (e, e'n) reactions are given. However, we intend mainly to stress the dominant factors for experimental feasibility rather than to propose a specific experiment.

First, the neutron electric form factor measurement will be examined assuming the experimentally found ratio of the ^{2}H(e, e'n) and (e, e'p) yields for the given kinematical conditions (see refs. 6 and 7).

The counting rate is evaluated with the following assumptions:

- $\Delta\Omega_e = 4.8 \times 10^{-3}$ sr corresponding to the maximum diaphragm available on the 900 spectrometer;
- $\Delta\Omega_n = 0.32 \times 10^{-3}$ sr, defined by the hole in the yoke of the 600 spectrometer;
- neutron detector efficiency $\eta = 0.10$;
- target thickness t = 250 mg/cm^2;
- average beam current $\langle I \rangle = 1\ \mu A$,

for the two kinematical conditions given in Table VII.

These conditions allow the linac to be operated at 2% duty-cycle (resulting in a better signal to noise ratio) or allow the 900 spectrometer to be set at the minimum scattering angle (resulting in a better counting rate).

As far as the accidental coincidences are concerned we point out that the ejected neutron and the scattered electron angles are respectively greater and lower than those given in Table V,

TABLE VII - The symbols have the usual meaning: Δt = time width of the true coincidence peak in the time of flight spectrum.

	p_e (MeV/c)	$p_{e'}$ (MeV/c)	$\vartheta_{e'}$ (°)	ϑ_n (°)	$\langle T_n \rangle$ (MeV)	ΔT_n (MeV)	Δt (ns)	Counts per hour
Kinematics I	400	377	29.5	68.8	21.0	22.2	43	250
Kinematics II	450	427	26.0	70.5	20.7	26.7	54	400

relative to the made measurements. Moreover the incident electron energy is lower. This implies a reduction by a factor of ~ 2 in the neutron arm rate and an increase by a factor of ~ 6 in the electron arm rate. Therefore, taking also into account the better duty-cycle, for the accidental counting rate, we take, for kinematics I the value measured at I = 1 μA, p_R = 0 MeV/c and s = 7.2 MeVee, that is 20 accidentals/(hour·ns). For the kinematics II, we consider a double value, that is 40 accidentals/(hour·ns).

Moreover if we measure simultaneously the (e, e'p) and the (e, e'n) cross sections σ, the σ(e, e'n) to σ(e, e'p) ratio is obviously not affected by changes in the electron arm efficiency. Then it is possible to use MPWC and thus to reduce the neutron time of flight peak width to ~ 3 ns whatever time of flight interval is accepted.

With these assumptions in the first kinematics the expected coincidence counting rate will be: N_{ev}/hour = 250 ± 17 (having assumed to deduce the accidental contribution in an interval of width twice the true peak); that is we can infer an accuracy of (6.7%)/hour. To have the required statistical precision of 1%[8] 45 hours of beam time are requested.

Analogously in the second kinematics we have: N_{ev}/hour = 400 ± 21, that is an accuracy of (5.4%)/hour. Therefore, to reach a 1% statistical accuracy, 29 hours are required.

Therefore, it is once again shown (see point d in ref. (1)) that the crucial point for this experiment is to determine the neutron detector absolute efficiency to within a 1% accuracy. This has been proved to be a difficult, but not impossible, task[9] and we stress that it does not necessarily require d.c. electron accelerators.

The second measurement examined is the ^{3}He(e, e'n) reaction. In knock-out reactions on three nucleons systems the residual two nucleons final system can be a singlet or a triplet isospin state. More precisely the measured spectral function S is decomposed into the T components of the residual system in the following way:

^{3}He(e, e'p) d
^{3}H (e, e'n) n, p
$\Rightarrow$ $S_1 = S_{T=0}(p, \omega = -2.22 \text{ MeV})$;
$\Rightarrow$ $S_2 = 3S_{T=0}(p, \omega > 0) + S_{T=1}(p, \omega > 0)$;

^{3}He(e, e'n) p, p
^{3}H (e, e'p) n, n
$\Rightarrow$ $S_3 = 2S_{T=1}(p, \omega > 0)$.

According to the Dieperink evaluation[10] the T=0 percentage in S_2 is about 20% at p = 0 MeV/c and increases to about 35% at p = 300 MeV/c. To separate the two components $S_{T=0}$ and $S_{T=1}$, the measurement of S_3 is required.

We consider the kinematical conditions used for S_1 and S_2 measurements to be the same as those used in the ^{3}He(e, e'p) reaction[11], that is:

- p_e = 530 MeV/c;
- ϑ_e = 52.2°;
- $\Delta\Omega_e$ = 4 x 10^{-3} sr;
- p_{transf} = 440 MeV/c;

- $\vartheta_n = 58^o$;
- $T_n = (82 - 110)$ MeV;
- $\Delta\Omega_n = 0.32 \times 10^{-3}$ sr.

We assume $\langle I \rangle = 1\ \mu A$; $t = 240$ mg/cm^2 and $\eta = 0.1$.

Taking the measured ^{3}He (e, e'p) three body break-up counting rate, the measured σ(e, e'p)/σ(e, e'n) ratio on deuterium, the evaluated spectral function values and the accidental rate measured at a threshold of 19.2 MeVee, the expected ^{3}He(e, e'n) counting rates are:

- at $p_R = 0$ MeV/c : N_{ev}/hour $\simeq 100 \pm 13$ (evaluated true to accidental ratio ~ 0.7); that is a 5 % accuracy in 7 hours of beam time;
- at $p_e = 100$ MeV/c: N_{ev}/hour $\simeq 15 \pm 9$ (evaluated true to accidental ratio ~ 0.1); that is a 10 % accuracy in 45 hours of beam time.

Finally we want to stress that the neutron detector efficiency and solid angle used in the previous considerations are lower by factors of 10 and 20 respectively than those of the usual proton detector. Therefore any effort in the direction of improving these values clearly would be very rewarding.

ACKNOWLEDGEMENTS.

It is our duty to thank Mr. R. Letourneau for his collaboration in assembling the experimental equipments, Mr. A. Mancieri for his help in the data analysis, and Mr. L. Pierangeli for his skill in drawing the figures.

REFERENCES.

(1) - P. Barreau, M. Bernheim, M. Brussel, G. P. Capitani, E. De Sanctis, J. M. Finn, S. Frullani, F. Garibaldi, E. Jans, J. Morgenstern, J. Mougey, D. Royer, D. Tarnowski, S. Turck-Chieze and P. Vernin, Istituto Superiore di Sanità, Internal Report ISS R 78/13 (1978).

(2) - P. Leconte, J. Mougey, A. Tomasso, P. Barreau, M. Bernheim, A. Bussiere de Nercy, L. Cohen, J. C. Comoretto, J. Dupont, S. Frullani, C. Grunberg, J. M. Hisleur, J. Le Dehevat, M. Lefevre, G. Lemarchand, J. Millaud, D. Royer and R. Salvaudon, Nuclear Instr. and Meth. 169, 401 (1980).

(3) - A. Bertin, A. Vitale and A. Placci, Nuclear Instr. and Meth. 68, 24 (1969).

(4) - G. Bianchi and J. P. Genin, CEA Internal Report (1972).

(5) - M. Anghinolfi, G. Ricco, P. Corvisiero and F. Marulli, Nuclear Instr. and Meth. 165, 217 (1979).

(6) - P. Bounnin, Nuclear Phys. 70, 401 (1965).

(7) - M. Gourdin, Phys. Rep. C11, 29 (1974).

(8) - H. Arenhövel, Y. E. Kim, B. A. Craver, W. Fabian and D. P. Saylor, Lett. Nuovo Cimento 23, 35 (1978).

(9) - G. Betti, A. Del Guerra, A. Giazotto, M. A. Giorgi, A. Stefanini, D. R. Botterill, D. W. Braben, D. Clarke and P. R. Norton, Nuclear Instr. and Meth. 135, 319 (1976).

(10) - A. E. L. Dieperink, T. De Forest Jr., I. Sick and R. A. Brandenburg, Phys. Letters 63B, 261 (1976); A. E. L. Dieperink, private communication.

(11) - J. Mougey, Proc. of "Few Body Systems and Electromagnetic Interactions", ed by. C. Ciofi degli Atti and E. De Sanctis, Lecture Notes in Physics (Springer, 1978), vol. 86, p. 305.